Used High Collimation UV-LEDs With a Miniaturized Optomechanical Device for the Detection of Direct Bilirubin

Zhi Ting Ye , *Senior Member, IEEE*, Shen Fu Tseng , Jun Yi Wu , and Hsin Ching Kuo

Abstract—Invasive blood testing is the most used method for testing bilirubin levels. However, invasive blood testing must be carried out by professionally trained medical staff to avoid the risk of infection. Apart from being present in blood, direct bilirubin is excreted in human urine. Therefore, this study proposed a non-invasive method, using high collimation ultraviolet-light-emitting diodes (HC UV-LEDs) as the light source to design a miniaturized optomechanical device (MOD) for direct bilirubin detection in urine. The designed MOD was used to analyze different concentrations of direct bilirubin using its absorbance spectrum to achieve a non-invasive detection method. The HC UV-LEDs MOD proposed in this study offers the benefits of being non-invasive and providing a quantitative analysis of direct bilirubin.

Index Terms—UV-LEDs, high collimation, non-invasive, direct bilirubin, quantitative analysis, coefficient of determination, miniaturized optomechanical device.

I. INTRODUCTION

BILIRUBIN, a yellow pigment, is produced by the catabolism of hemoglobin in red blood cells. Normally, bilirubin circulates to the liver through the blood combined with uridine 5'-diphospho-glucuronosyltransferase and is excreted into the intestine with bile before finally being converted into urobilinogen, which is excreted in the urine and feces. The bilirubin before and after binding with liver cells is called indirect (unconjugated) and direct (conjugated) bilirubin, respectively. Total bilirubin is the sum of indirect and direct bilirubin [1], [2], [3]. A high index value of indirect bilirubin can affect brain development due to a clinical condition called jaundice (hyperbilirubinemia). Jaundice is a consequence of the liver cells not converting indirect bilirubin to direct bilirubin in a short time, resulting in an excessively high indirect bilirubin index in the blood. If the direct bilirubin index is too high, clinically

called bile retention (conjunctive jaundice; bileretentive jaundice), neonates can develop biliary atresia [4], [5], [6], which is medically called neonatal jaundice. Neotal jaundice affects 60% and 80% of full-term neonates and preterm neonates, respectively. As a result, bilirubin testing is a regular procedure performed on newborns [7], [8].

Newborns often have jaundice because the liver is not fully developed, so the liver cells lack the ability to bind bilirubin. When the body's function of binding bilirubin matures, this problem will disappear, resulting in physiologic jaundice [9], [10], [11]. Physiologic jaundice will last one to two weeks; it appears on the second day of life, peaks on the fourth to fifth day, and then subsides. In addition, neonates may develop pathological jaundice (combined jaundice; cholestatic jaundice) due to hepatitis or biliary atresia. In biliary atresia, early diagnosis and surgery are necessary to avoid the eventual need for a liver transplant. If the bilirubin index is too high for a long time, it may lead to conditions, such as athetosis, hearing loss, and mental deficiencies [12], [13]. In addition, high concentrations of bilirubin may cause biliary duct or hepatic dysfunction, brain damage, or even death [14], [15], [16].

Neonatal jaundice lasting more than two weeks is clinically called delayed jaundice and should be investigated to confirm if the cause is pathological jaundice. When delayed jaundice is present in a newborn, the American Academy of Pediatrics (AAP) recommends drawing blood for total and direct bilirubin testing to rule out the possibility of biliary atresia. In Taiwan, to detect biliary atresia in newborns, parents are provided a stool color card in the health handbook to compare their infant's stool color for early biliary atresia screening. However, comparing infants' stools with the stool color cards is subjective and raises concerns about making errors. Therefore, it is hoped that developing a non-invasive urine bilirubin test to provide accurate and immediate results will assist parents and health workers.

Currently, the most widely used detection method for bilirubin in clinical medicine is the diazotization (diazo) method. The traditional diazo method combines serum and diazonium reagents into diazonium salts at pH 1.7–2.0. The diazonium salts react with bilirubin to form azobilirubin, which has an absorbance intensity at the wavelength of 600 nm. The absorbance reading is proportional to the direct bilirubin concentration [17]. Various diazo methods have been developed to determine the direct bilirubin [18], [19]. However, the diazo reagent is unstable

and must be synthesized from sodium nitrite and aminobenzenesulfonic acid, and is easily affected by pH [20], [21]. In addition, neonatal serum has a high rate of hemolysis, which leads to deviations in the detection results, and may affect timely treatment [22]. Bilirubin oxidase is a multicopper oxidase enzyme that belongs to the oxidoreductase class of enzymes. It catalyzes the oxidation of bilirubin to biliverdin. This enzyme has been broadly utilized as a test reagent [23], [24]. Bilirubin is oxidized by bilirubin oxidase under acidic conditions to produce biliverdin, which is used to determine the bilirubin concentration [25]. In addition, some oxidase methods were used to determine the direct bilirubin [26], [27], [28], [29] However, oxidase methods for detecting bilirubin, have several disadvantages, such as low sensitivity, high cost, and low stability [30], [31], [32].

Fluorescence detection has attracted much attention due to its good optical properties; it provides a fast response, high selectivity, amplified sensitivity, and a wide range of concentrations [33], [34], [35]. The determine of direct bilirubin by fluorescence methods have the advantage of low response times [36], [37], [38]. Howerer, the used of fluorescence to detect substances without interferers delivers good detection results, but for samples with complex components, such as urine and blood, there is interference [39], [40]. Normally, bilirubin is excreted from the body, and only a small amount of bilirubin exists in the blood and urine. However, when biliary atresia or hepatitis occurs, the direct bilirubin in the blood cannot be converted efficiently and excreted out of the body, so the concentration of direct bilirubin will increase. Only direct bilirubin can dissolve in water and be excreted in the urine after passing through the kidneys. Therefore, early assessments can be made by detecting direct bilirubin concentrations in the urine [41], [42]. In recent years, scholars have also conducted direct analysis and research on bilirubin and absorption spectra [43], [44]. Direct bilirubin detection using spectral analysis RGB Mini-LED as light source. High collimation light sources can achieve relatively smaller spot sizes, enhancing the efficiency of light incident on the test object and reducing the occurrence of stray light, thus significantly aiding in improving linearity [45]. The recent progress in electrochemical and optical biosensors for monitoring SARS-CoV-2 and various pathogens [46]. UV LEDs are gradually becoming more prevalent in biomedical applications, with research on their optoelectronic properties cited in [47], [48], [49].

The current methods for detecting bilirubin mainly detect total, direct, and indirect bilirubin in blood. Since direct bilirubin can be excreted in urine, this study proposed us-ing high collimation ultraviolet-light-emitting diodes (HC UV-LEDs) as the light source, to design a miniaturized optomechanical device (MOD) to determine direct bilirubin in urine. The fabricated HC UV-LEDs MOD was used to analyze direct bilirubin concentrations range from 8.55 to 350.55 μmol/L using its absorbance spectrum. The linear regression was y = 0.0034x + 0.1686, R^2 value was 0.9983, the LOD of 35.167 μmol/L, the LOQ of 117.225 μmol/L which offers the benefits of being non-invasive, fast, and providing a digital quantitative analysis.

II. MATERIALS AND METHODS

A. Direct Bilirubin Sample

This article used the Direct Bilirubin Sample with the bilirubin standard kit List No. 9450. (Verichem Laboratories, Inc., Rhode Island, USA) is the reference standard for direct bilirubin in clinical laboratories and intended specifically for calibration verification. The CAS certification number is 68683-34-1. Five different direct bilirubin concentrations, 8.55, 94.05, 179.55, 265.05, and 350.55 μmol/Lwere pre-processed in a sterile box before measuring the spectrum. First, the direct bilirubin was mixed uniformly by stirring at 500 rpm for 5 minutes using a magnetic stirrer. Then a 50 μm/L sample of direct bilirubin was pipetted into the quartz cell using a variable volume (S Series Micropipette MS-100H, Taichung, Taiwan) to fill a quartz cell and measure the absorbance spectrum.

B. Design of the Miniaturized Optomechanical Device

In order to enhance portability and improve ease of use for patients, the MOD was developed as a detection instrument. The deployment process is shown in Fig. 1(a). In this experiment, a quartz cell was used as the measurement container. Compared with ordinary glass, the absorbance value of quartz in the ultraviolet (300–380 nm) band and visible light band (400–700 nm) is minimal. The absorbance values measured for the 300–600 nm band are less than 0.063, which means that most of the light can penetrate, reducing the measurement error, as shown in Fig. 1(b). The MOD comprises a light source (high collimation ultraviolet-light-emitting diodes (HC UV-LEDs), collimating lens$_{in}$, fiber, collimating lens$_{out}$, and micro spectrometer as shown in Fig. 1(c).

The focal lengths of lens$_{in}$ and lens$_{out}$ can be calculated by (1):

$$\frac{1}{f} = \left(\frac{n}{n_i} - 1\right)\left[\frac{1}{R_1} - \frac{1}{R_2} + \frac{(n-1)\,d}{n R_1 R_2}\right] \quad (1)$$

The f represents the focal length of the lens, while n stands for the refractive index of the lens material. n_i denotes the refractive index of the material surrounding the lens material. R_1 represents the radius of curvature of the lens surface near the light source, whereas R^2 represents the radius of curvature of the lens surface on the opposite side. Lastly, d corresponds to the thickness of the lens and the material is quartz.

The HC UV-LEDs MOD proposed in this study for detecting direct bilirubin uses the Beer-Lambert Law to analyze the absorbance e and determine the concentration. The Beer-Lambert law formula derivation process is shown in (2) and (3).

$$T = \frac{I_1}{I_0} \quad (2)$$

$$A = log_{10}\left(\frac{I_0}{I_1}\right) = \varepsilon \cdot \ell \cdot c \quad (3)$$

Where T is the light transmittance, A is the sample's absorbance of the sample, I_0 is the incident light intensity, I_1 is the transmitted light intensity, ε is the absorbance coefficient of

(a)

Pre-processing in a sterile box   Magnetic stirring   Filling into a quartz cell
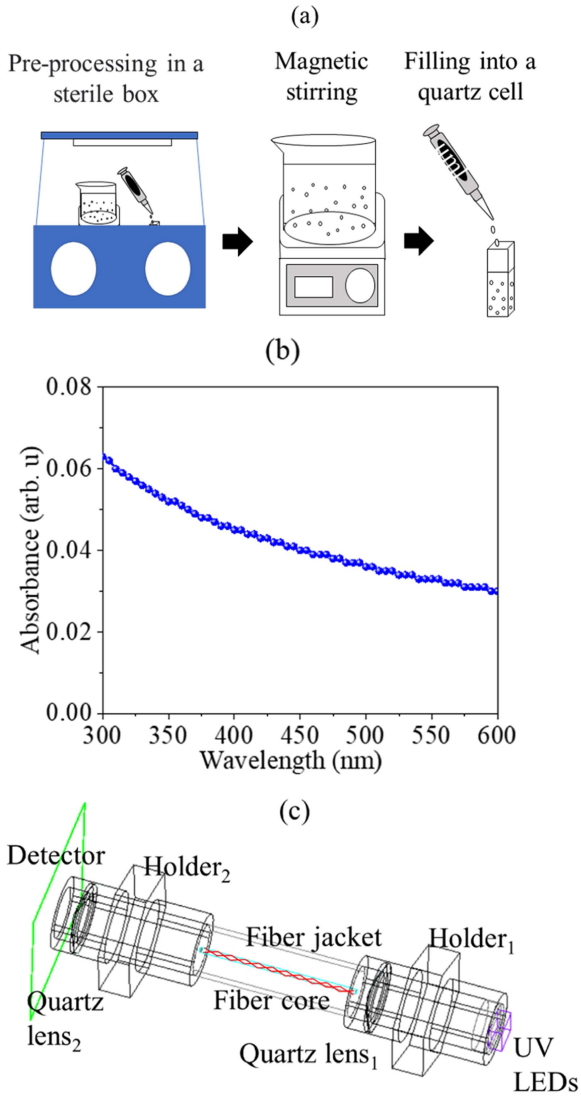

(b)

(c)

Fig. 1. Design of the miniaturized optomechanical device detect bilirubin (a) the flow diagram of direct bilirubin sample preparation. (b) The absorbance spectrum (300–600 nm) for the quartz cell. (c) UV LED MOD architecture.

the absorbin0g substance, ℓ is the absorbing medium thickness (cm), and c is the absorbing substance concentration (μmol/L).

C. Experimental Process

In this study, we proposed using a light source to design a MOD for detecting direct bilirubin. Step 1: Initially, five different concentrations of direct bilirubin standard solutions from 8.55 to 350.55 μmol/L were prepared, and the absorbance of air was used as the baseline to zero-calibrate the spectrometer (Model U-3900, Hitachi, Ltd., Tokyo, Japan,). Step 2: Measure the absorbance value of 5 different concentrations of direct bilirubin, analyze the linear relationship between the absorbance value and the concentration were measured in, and find the optimum fitting region. Step 3: Analyze the relationship of the optimum fitting region between direct bilirubin concentration and absorbance, and find the wavelength with the optimum linearity through the binary linear regression and the R^2 value.

Step 4: Conduct a reproducibility experiment, repeat the erection of the selfmade MOD five times, and analyze the average standard error of detecting direct bilirubin. Step 5: Finally, the results from the fabricated MOD and the Hitachi U-3900 spectrometer were compared to verify the MOD designed for this study's ability to detect direct bilirubin. The MOD experiments will fix the integration time of the micro spectrometer and test in the dark room with a room temperature and humidity of 25 °C and 60%, respectively.

III. MATERIALS AND METHODS

A. Direct Bilirubin Absorbance Spectrum Analysis

In order to ensure the absorbance band of MOD analysis direct bilirubin in the follow-up experiment, direct bilirubin was first measured by a Hitachi U-3900 spectrometer; the absorbance value was measured at a scan rate of 2 nm/s, slit 2 nm, and PMT 200 V. Five different concentrations of direct bilirubin were prepared (8.55, 94.05, 179.55, 265.05, and 350.55 μmol/L), and their absorbance values measured as shown in Fig. 2(a), the first absorbance peak (FA$_P$) and second absorbance peak (SA$_P$) are 300 nm and 400 nm, respectively. The optimum fitting region was found in the 300–400 nm absorbance band, and the R^2 values reached above 0.99 as shown in Fig. 2(b).

In Fig. 2(c) shows the linearity analysis of direct bilirubin for the concentration range of 8.55 to 350.55 μmol/L at 350 nm. The linear regression is y = 0.003x + 0.1999, and the R^2 value was 0.999. The wavelength 400 nm is the second absorbance peak (SA$_P$): the linear relationship is shown in Fig. 2(d). The experimental results show that at 400 nm in the direct bilirubin concentration range of 8.55 to 350.55 μmol/L; the linear regression is y = 0.004x + 0.0431, and the R^2 value reached 0.9908.

When direct bilirubin concentrations between 8.55 and 350.55 μmol/L analyzed using a Hitachi U 3900 double-beam UV/Vis spectrometer had an excellent linear relationship in the 300 to 450 nm wavelength bands. The wavelength of 350 nm was the optimal fitting wavelength in this concentration range, with R^2 values up to 0.999. The Hitachi U3900 spectrometer was found to have excellent accuracy and detection tolerance, but it is inconvenient to carry due to its size. Therefore, we fabricated and evaluated a MOD using HC UV-LEDs as a light source.

B. Detecting Direct Bilirubin by Using the Fabricated HC UV-LEDs MOD

After confirming the absorption band of the albumin, HC UV-LEDs MOD will be developed through FC UVC LEDs to reduce the size of the instrument. The prototype HC UV-LEDs MOD developed in this study was 3.5, 3.5, and 2 mm in length, width, and height, respectively. Fig. 3(a) shows the prototype of UV-LEDs MOD. The optomechanical device was custom-designed and machined using Computer Numerical Control (CNC) processing to secure the relative positions of the light source, fiber, lens$_{in}$, Quartz cell, and lens$_{out}$. The material used is aluminum (5051) with a surface finish of hard-baked black paint. The micro spectrometer of model SE1030-025-FUVN, produced by OtO
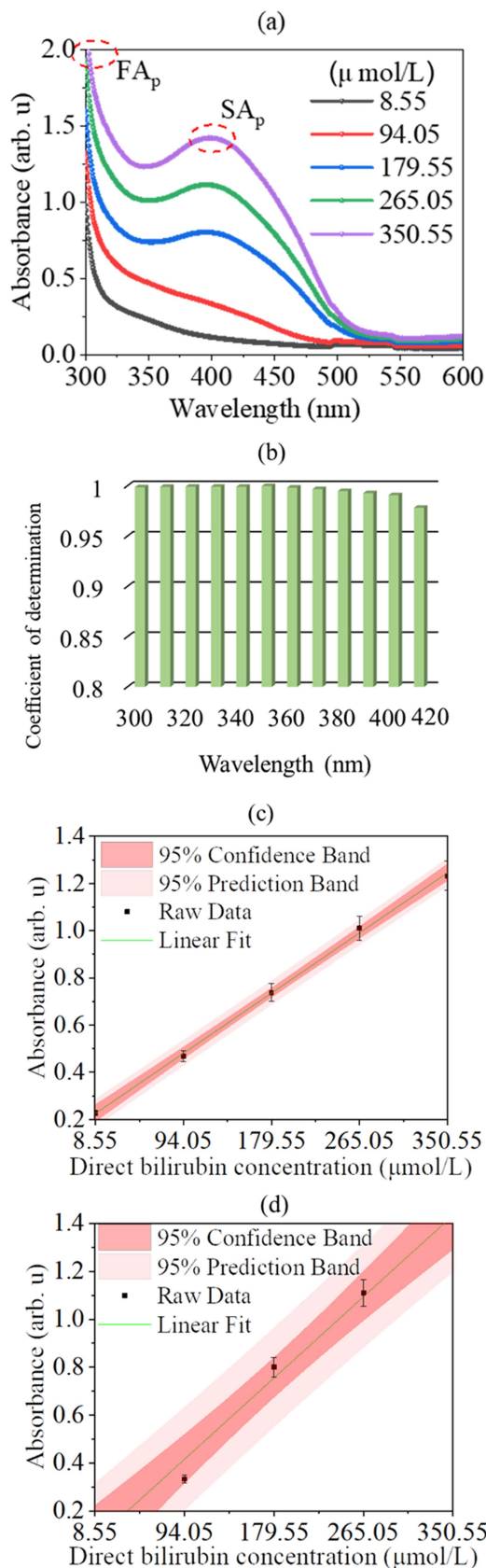
Fig. 2. Absorbance spectrum of direct bilirubin using a Hitachi U-3900 spectrometer. (a) Absorbance spectrum. (b) The linear relationship in the 300 to 450 nm wavelength bands. (c) The linear analysis of direct bilirubin at 350 nm. (d) The linear analysis of direct bilirubin at 400 nm.
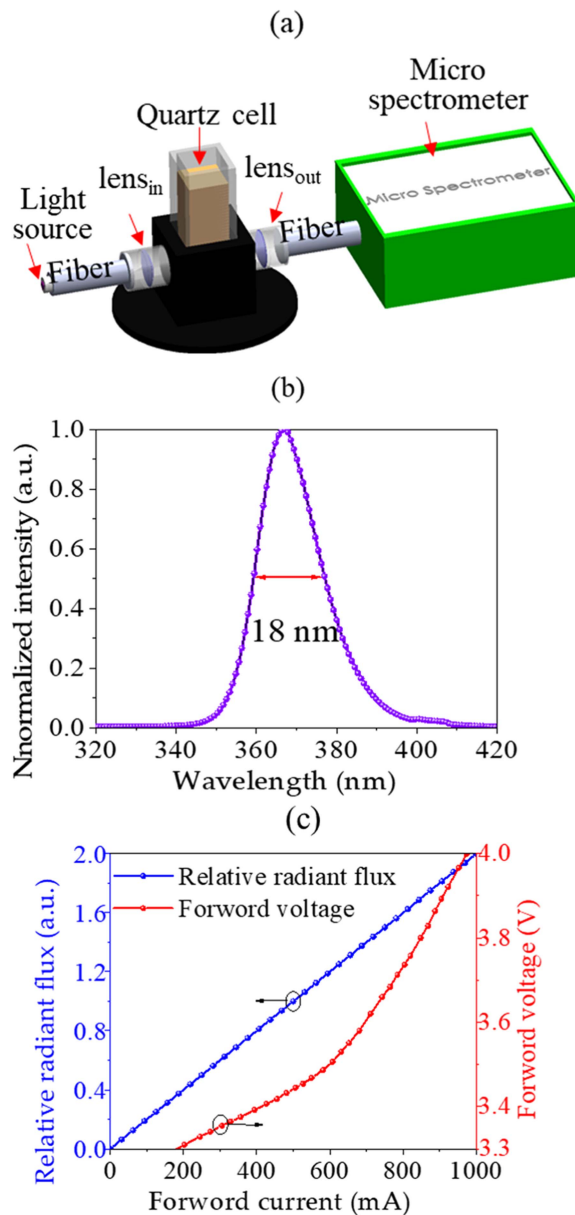

Fig. 3. HC UV-LEDs MOD developed (a) the prototype of UV-LEDs MOD, entity diagram of the miniature optical system (MOS) with FC UV-LEDs. (b) Emission spectra of UV-LEDs, and (c) measured light-current-voltage (L-I-V) curve.

Photonics, Inc., Hsinchu City, Taiwan. The drive conditions of the UV-LEDs were 3.35 V 300 mA. The emission spectrum is shown in Fig. 3(b). There is a maximum peak at 365 nm, including the optimal linearity wavelength of 350 nm. The full width at half maximum (FWHM) of the spectrum is 18 nm. Fig. 3(c) is the measured light-current-voltage (L-I-V) curve. The inflection point in the UV LED LIV curve between 600mA and 800mA is usually the result of a combination of changes in internal excitation mechanisms, thermal effects, and optical effects.

The optical fiber used had a numerical aperture of 0.22, core size of 600 μm, and a length of 30 cm. The back focal length of the collimating lens was 10 mm and the numerical aperture was

TABLE I
REPRODUCIBILITY MEASUREMENT OF THE HC UV-LED MOD

Direct bilirubin Concentration (μmol/L)	The absorbance for the first test (arb. u)	The absorbance for a second test (arb. u)	The absorbance for the third test (arb. u)	The absorbance for the fourth test (arb. u)	The absorbance for the fifth test (arb. u)	Standard error (%)
8.55	0.217	0.216	0.217	0.216	0.215	0.04
179.55	0.783	0.783	0.787	0.786	0.785	0.08
350.55	1.367	1.366	1.363	1.363	1.373	0.18

0.22. The light absorbed through the quartz cell was converted into parallel light by a collimating lens before it entered the optical fiber. Finally, different direct bilirubin concentrations were analyzed by a micro spectrometer (Model SE1030-025-FUVN, OtO Photonics, Inc., Hsinchu City, Taiwan).

The direct bilirubin concentrations measured by the Hitachi U-3900 spectrometer, identified that the optimal fitting range was in the wavelength band of 300 to 400 nm and that the optimal linear wavelength was 360 nm. Therefore, this study's fabricated HC UV-LEDs MOD was used in the 320 to 390 nm wavelength band to analyze the relationship between direct bilirubin absorbance and wavelength. In order to enhance the collimated MOD of the light source, fiber and lens are used to design the HC UV-LEDs MOD. Fig. 4(a) is the polar candela distribution plot of UV- LEDs, UV- LEDs with fiber, and UV- LEDs with fiber and $lens_{in}$, the half-intensity angle are 60 degrees, 12.5 degree and, and 1 degree, respectively. In Fig. 4(b) represents the standard emission pattern of UV LEDs commonly used in the industry with a half-intensity angle of 60 degrees. In Fig. 4(c), UV-LEDs with fiber exhibit a half-intensity angle of 12.5 degrees. In Fig. 4(d), UV-LEDs with fiber, $lens_{in}$ and $lens_{out}$ that can reduce the half-intensity angle to 1 degree. Fig. 4(e) is the absorbance spectrum of five concentrations of direct bilirubin measured using the HC UV-LEDs MOD. The best fitting wavelength was identified as 360 nm as shown in Fig. 4(f), the linear regression was y = 0.0034x + 0.1686, and the R^2 value was 0.9983, the LOD of 35.167 μmol/L, and the LOQ of 117.225 μmol/L.

Next, a reproducibility test was conducted. The HC UV-LEDs MOD was rebuilt five times, and each was used to measure three different concentrations of direct bilirubin at 360 nm; the highest concentration was 350.55 μmol/L, the median concentration was 179.55 μmol/L, and the lowest concentration was 8.55 μmol/L. The experimental results are shown in Table I. The standard error of the absorbance intensity at 360 nm for the 350.55, 179.55, and 8.55 μmol/L direct bilirubin concentrations was 0.04%, 0.08%, and 0.18%, respectively, and the average standard error was 0.1%. According to these experimental results, the HC UV-LEDs MOD demonstrated excellent reproducibility in the
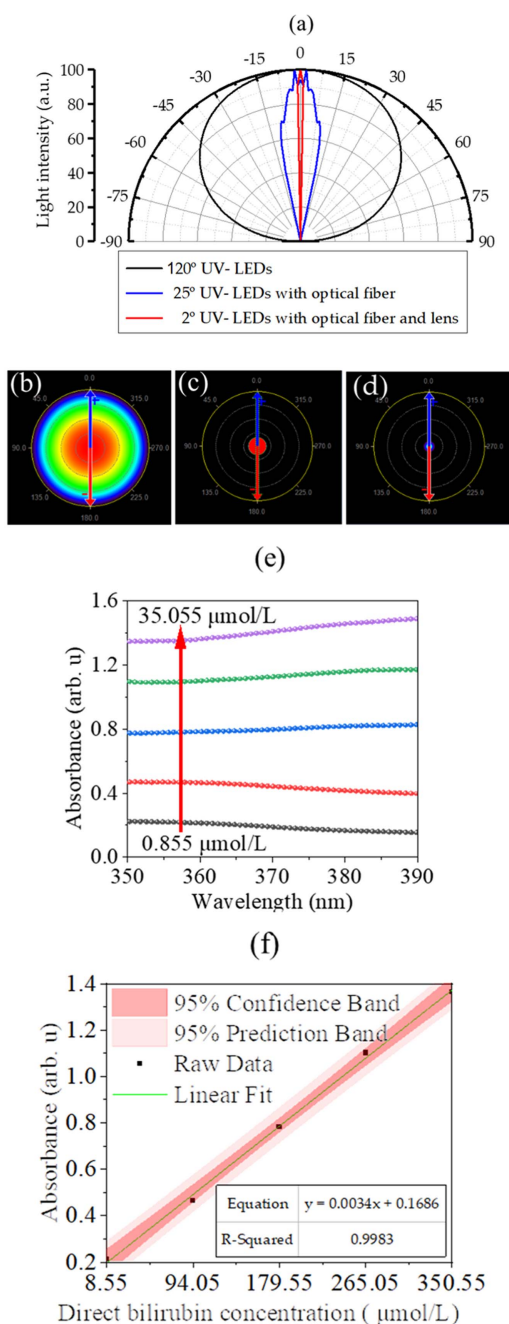
Fig. 4. Absorbance spectrum of five concentrations of direct bilirubin measured using the HC UV-LEDs MOD. (a) Polar candela distribution plot (b) angular profiles of the UV-LEDs, (c) UV-LEDs with fiber, and (d) UV-LEDs with fiber and collimating $lens_{in}$. (e) Absorbance spectrum. (f) The linear analysis of the absorbance of direct bilirubin at 360 nm.

repeated fabrication test and the measurement of direct bilirubin concentration at 360 nm.

Compare the measurement results of the HC UV-LED MOD proposed in this article and the Hitachi U-3900 spectrometer, the direct bilirubin standard solution's concentrations were measured with the HC UV-LEDs MOD, and the linear relationship was analyzed between the concentration and the transmission spectrum. The results show that the best fitting band for direct bilirubin concentrations from 8.55 to 350.55 μmol/L is 360 nm,

the linear regression was found to be y = 0.0034x + 0.1686, and the R^2 value was 0.9983. The Hitachi U-3900 spectrometer was used to measure direct bilirubin concentrations from 0.855 to 35.055 μmol/L at 350 nm. The linear regression was found to be y = 0.003x + 0.1999, and the R^2 value was 0.999. These results support that there is good agreement between the two methods.

IV. CONCLUSION

The experimental results show that the UV-LEDs MOD developed in this study and Hitachi U-3900 spectrometer have an excellent linear relationship when detecting direct bilirubin between the concentrations of 8.55 to 350.55 μmol/L, and the optimal fitting wavelength for Hitachi U-3900 and UV-LEDs MOD is 350 nm and 360 nm, respectively.

This study proposed a non-invasive spectroscopic detection method to detect direct bilirubin. The fabricated HC UV-LEDs MOD and the Hitachi U-3900 spectrometer were used to analyze the relationship between direct bilirubin at different concentrations and the light absorbance change in the spectrum. Linear regression analysis of the HC UV-LEDs MOD's results showed that direct bilirubin concentration corresponded to the absorbance values to achieve a non-invasive direct bilirubin quantitative analysis. The experimental results showed that the HC UV-LEDs MOD's optimal fitting wavelength to detect direct bilirubin concentrations from 8.55 to 350.55 μmol/L is 360 nm, the R^2 value was 0.9983, the LOD of 35.167 μmol/L, and the LOQ of 117.225 μmol/L. The average standard error of measurement reproducibility was 0.1%. Comparing the blue HC UV-LEDs MOD at 360 nm and the Hitachi U-3900 spectrometer at 350 nm, detect different concentrations of direct bilirubin, the linear regression and R^2 values are y = 0.0034x + 0.1686, 0.9983 and y = 0.003x + 0.1999, 0.999, respectively. The HC UV-LEDs MOD can effectively simplify the measurement of direct bilirubin, it demonstrated high accuracy while achieving non-invasive quantitative detection of direct bilirubin in urine. Therefore, the HC UV-LEDs MOD have the advantage such as portability and small size. In the future, the highly portable device can be used as a non-invasive direct bilirubin detection method for medical use, providing a more convenient detection method for patients with jaundice.

REFERENCES

[1] Q. Yao, R. Chen, V. Ganapathy, and L. Kou, "Therapeutic application and construction of bilirubin incorporated nanoparticles," *J. Controlled Release*, vol. 328, pp. 407–424, 2020.

[2] P. Y. Kwo, S. M. Cohen, and J. K. Lim, "ACG clinical guideline: Evaluation of abnormal liver chemistries," *Official J. Amer. College Gastroenterol.*, vol. 112, no. 1, pp. 18–35, 2017.

[3] A.-R. Hamoud, L. Weaver, D. E. Stec, and T. D. Hinds, "Bilirubin in the liver–gut signaling axis," *Trends Endocrinol. Metab.*, vol. 29, no. 3, pp. 140–150, 2018.

[4] L. Vítek, "Bilirubin as a signaling molecule," *Med. Res. Rev.*, vol. 40, no. 4, pp. 1335–1351, 2020.

[5] M. Hjelkrem, A. Morales, C. Williams, and S. Harrison, "Unconjugated hyperbilirubinemia is inversely associated with non-alcoholic steatohepatitis (NASH)," *Alimentary Pharmacol. Therapeutics*, vol. 35, no. 12, pp. 1416–1423, 2012.

[6] K.-H. Wagner, R. G. Shiels, C. A. Lang, N. S. Khoei, and A. C. Bulmer, "Diagnostic criteria and contributors to Gilbert's syndrome," *Crit. Rev. Clin. Lab. Sci.*, vol. 55, no. 2, pp. 129–139, 2018.

[7] R. Cayabyab and R. Ramanathan, "High unbound bilirubin for age: A neurotoxin with major effects on the developing brain," *Pediatr. Res.*, vol. 85, no. 2, pp. 183–190, 2019.

[8] J. G. Bell, M. P. Mousavi, M. K. A. El-Rahman, E. K. Tan, S. Homer-Vanniasinkam, and G. M. Whitesides, "based potentiometric sensing of free bilirubin in blood serum," *Biosensors Bioelectron.*, vol. 126, pp. 115–121, 2019.

[9] B. O. Olusanya, M. Kaplan, and T. W. Hansen, "Neonatal hyperbilirubinaemia: A global perspective," *Lancet Child Adolesc. Health*, vol. 2, no. 8, pp. 610–620, 2018.

[10] T. W. Hansen, R. J. Wong, and D. K. Stevenson, "Molecular physiology and pathophysiology of bilirubin handling by the blood, liver, intestine, and brain in the newborn," *Physiol. Rev.*, vol. 100, no. 3, pp. 1291–1346, 2020.

[11] A. M. Armanian, S. Jahanfar, A. Feizi, N. Salehimehr, M. Molaeinezhad, and E. Sadeghi, "Prebiotics for the prevention of hyperbilirubinaemia in neonates," *Cochrane Database Systematic Rev.*, vol. 8, no. 8, 2019, Art. no. CD012731.

[12] F. Ebbesen, P. K. Vandborg, and M. L. Donneborg, "The effectiveness of phototherapy using blue-green light for neonatal hyperbilirubinemia–Danish clinical trials," *Seminars Perinatology*, vol. 45, no. 1, 2021, Art. no. 151358.

[13] J. F. Watchko and M. J. Maisels, "The enigma of low bilirubin kernicterus in premature infants: Why does it still occur, and is it preventable?," *Seminars Perinatology*, vol. 38, no. 7, pp. 397–406, 2014.

[14] C. Song et al., "A novel anticoagulant affinity membrane for enhanced hemocompatibility and bilirubin removal," *Colloids Surfaces B: Biointerfaces*, vol. 197, 2021, Art. no. 111430.

[15] W. Xiao, D. Zhi, Q. Pan, Y. Liang, F. Zhou, and Z. Chen, "A ratiometric bilirubin sensor based on a fluorescent gold nanocluster film with dual emissions," *Anal. Methods*, vol. 12, no. 47, pp. 5691–5698, 2020.

[16] C. Zhang, W. Bai, T. Qin, and Z. Yang, "Fabrication of red mud/molecularly imprinted polypyrrole-modified electrode for the piezo-electric sensing of bilirubin," *IEEE Sensors J.*, vol. 19, no. 4, pp. 1280–1284, Feb. 2019.

[17] N. Dhungana, C. Morris, and M. D. Krasowski, "Operational impact of using a vanadate oxidase method for direct bilirubin measurements at an academic medical center clinical laboratory," *Practical Lab. Med.*, vol. 8, pp. 77–85, 2017.

[18] R. P. Edachana, A. Kumaresan, V. Balasubramanian, R. Thiagarajan, B. G. Nair, and S. B. T. Gopalakrishnan, "Based device for the colorimetric assay of bilirubin based on in-situ formation of gold nanoparticles," *Microchimica Acta*, vol. 187, pp. 1–9, 2020.

[19] I. M. Lano, A. W. Lyon, L. Wang, R. Ruskin, and M. E. Lyon, "Comparative evaluation of neonatal bilirubin using radiometer whole blood co-oximetry and plasma bilirubin methods from Roche Diagnostics and Ortho Clinical Diagnostics," *Clin. Biochem.*, vol. 53, pp. 88–92, 2018.

[20] C.-Y. Li, S. H.-J. Hsu, C.-C. Chang, and G.-J. Wang, "Direct bilirubin detection using surface-enhanced Raman spectroscopy," *IEEE Sensors J.*, vol. 21, no. 19, pp. 21458–21464, Oct. 2021.

[21] W. Tan, L. Zhang, J. C. Doery, and W. Shen, "Study of paper-based assaying system for diagnosis of total serum bilirubin by colorimetric diazotization method," *Sensors Actuators B: Chem.*, vol. 305, 2020, Art. no. 127448.

[22] M. Devgun and C. Richardson, "Direct bilirubin in clinical practice—Interpretation and haemolysis interference guidance reassessed," *Clin. Biochem.*, vol. 49, no. 18, pp. 1351–1353, 2016.

[23] R. Rawal, P. R. Kharangarh, S. Dawra, M. Tomar, V. Gupta, and C. Pundir, "A comprehensive review of bilirubin determination methods with special emphasis on biosensors," *Process Biochem.*, vol. 89, pp. 165–174, 2020.

[24] B. Thangavel, J. Lingagouder, S. Berchmans, and V. Ganesh, "Electrochemical grafting of 4-aminobenzoic acid onto toray carbon–Interfacial investigation and fabrication of non-enzymatic bilirubin sensor," *Sensors Actuators B: Chem.*, vol. 344, 2021, Art. no. 130292.

[25] H. Okada et al., "Effects of bilirubin photoisomers on the measurement of direct bilirubin by the bilirubin oxidase method," *Ann. Clin. Biochem.*, vol. 55, no. 2, pp. 276–280, 2018.

[26] R. Rawal, P. R. Kharangarh, S. Dawra, and P. Bhardwaj, "Synthesis, characterization and immobilization of bilirubin oxidase nanoparticles (BOxNPs) with enhanced activity: Application for serum bilirubin determination in jaundice patients," *Enzyme Microbial Technol.*, vol. 143, 2021, Art. no. 109716.

[27] S. Iwatani et al., "A novel method for measuring serum unbound bilirubin levels using glucose oxidase-peroxidase and bilirubin-inducible fluorescent protein (UnaG): No influence of direct bilirubin," *Int. J. Mol. Sci.*, vol. 21, no. 18, 2020, Art. no. 6778.

[28] R. Rawal, N. Chauhan, M. Tomar, and V. Gupta, "A contrivance based on electrochemical integration of graphene oxide nanoparticles/nickel nanoparticles for bilirubin biosensing," *Biochem. Eng. J.*, vol. 125, pp. 238–245, 2017.

[29] N. Chauhan, R. Rawal, V. Hooda, and U. Jain, "Electrochemical biosensor with graphene oxide nanoparticles and polypyrrole interface for the detection of bilirubin," *Roy. Soc. Chem. Adv.*, vol. 6, no. 68, pp. 63624–63633, 2016.

[30] L. Ouyang, L. Yao, R. Tang, X. Yang, and L. Zhu, "Biomimetic point-of-care testing of trace free bilirubin in serum by using glucose selective capture and surface-enhanced Raman spectroscopy," *Sensors Actuators B: Chem.*, vol. 340, 2021, Art. no. 129941.

[31] Y. Du, X. Li, X. Lv, and Q. Jia, "Highly sensitive and selective sensing of free bilirubin using metal–organic frameworks-based energy transfer process," *Amer. Chem. Soc. Appl. Mater. Interfaces*, vol. 9, no. 36, pp. 30925–30932, 2017.

[32] X. Pan et al., "A graphene oxide-gold nanostar hybrid based-paper biosensor for label-free SERS detection of serum bilirubin for diagnosis of jaundice," *Biosensors Bioelectron.*, vol. 145, 2019, Art. no. 111713.

[33] C. Xia et al., "An ultrafast responsive and sensitive ratiometric fluorescent pH nanoprobe based on label-free dual-emission carbon dots," *J. Mater. Chem. C*, vol. 7, no. 9, pp. 2563–2569, 2019.

[34] S. Nandi and S. Biswas, "A recyclable post-synthetically modified Al (iii) based metal–organic framework for fast and selective fluorogenic recognition of bilirubin in human biofluids," *Dalton Trans.*, vol. 48, no. 25, pp. 9266–9275, 2019.

[35] R. Anjana et al., "S, N-doped carbon dots as a fluorescent probe for bilirubin," *Microchimica Acta*, vol. 185, pp. 1–11, 2018.

[36] M. Jayasree et al., "Fluorescence turn on detection of bilirubin using Fe (III) modulated BSA stabilized copper nanocluster; a mechanistic perception," *Analytica Chimica Acta*, vol. 1031, pp. 152–160, 2018.

[37] W. Zhao et al., "Ultrasensitive free bilirubin detection in whole blood via counting quantum dots aggregates at single nanoparticle level," *Sensors Actuators B: Chem.*, vol. 275, pp. 95–100, 2018.

[38] C. Xia et al., "A selective and sensitive fluorescent probe for bilirubin in human serum based on europium (III) post-functionalized Zr (IV)-based MOFs," *Talanta*, vol. 212, 2020, Art. no. 120795.

[39] E. Ahmmed et al., "Bilirubin quantification in human blood serum by deoxygenation reaction switch-triggered fluorescent probe," *Amer. Chem. Soc. Appl. Bio Mater.*, vol. 3, no. 7, pp. 4074–4080, 2020.

[40] J. T.-H. Yeh, K. Nam, J. T.-H. Yeh, and N. Perrimon, "eUnaG: A new ligand-inducible fluorescent reporter to detect drug transporter activity in live cells," *Sci. Rep.*, vol. 7, no. 1, 2017, Art. no. 41619.

[41] K. Ponhong, N. Teshima, K. Grudpan, S. Motomizu, and T. Sakai, "Simultaneous injection effective mixing analysis system for the determination of direct bilirubin in urinary samples," *Talanta*, vol. 87, pp. 113–117, 2011.

[42] P. Resmi, J. Raveendran, P. Suneesh, T. Ramanchandran, B. G. Nair, and T. S. Babu, "Screen-printed carbon electrode for the electrochemical detection of conjugated bilirubin," *Mater. Lett.*, vol. 304, 2021, Art. no. 130574.

[43] O. F. Laterza, C. H. Smith, T. R. Wilhite, and M. Landt, "Accurate direct spectrophotometric bilirubin measurement combined with blood gas analysis," *Clinica Chimica Acta*, vol. 323, no. 1/2, pp. 115–120, 2002.

[44] H. A. Lee et al., "Direct bilirubin is more valuable than total bilirubin for predicting prognosis in patients with liver cirrhosis," *Gut Liver*, vol. 15, no. 4, pp. 599–605, 2021.

[45] Z. T. Ye, S. F. Tseng, S. X. Tsou, and C. W. Tsai, "Spectral analysis with highly collimated mini-LEDs as light sources for quantitative detection of direct bilirubin," *Discover Nano*, vol. 19, no. 1, 2024, Art. no. 13.

[46] S. Ahmed et al., "Electrochemical and optical-based systems for SARS-COV-2 and various pathogens assessment," *Adv. Natural Sci.: Nanoscience Nanotechnol.*, vol. 14, 2023, Art. no. 033001.

[47] M. A. Sahar, Z. Hassan, S. S. Ng, and N. A. Hamzah, "Highly efficient near ultraviolet LEDs using InGaN/GaN/AlxGa1-xN/GaN multiple quantum wells at high temperature on sapphire substrate," *Mater. Sci. Semicond. Process.*, vol. 156, 2023, Art. no. 107298.

[48] Y. Wang, R. Chen, D. Liu, C. Peng, J. Wang, and X. Dong, "New functionalized thioxanthone derivatives as type I photoinitiators for polymerization under UV-Vis LEDs," *New J. Chem.*, vol. 47, no. 11, pp. 5330–5337, 2023.

[49] R. Xu, Q. Kang, Y. Zhang, X. Zhang, and Z. Zhang, "Research progress of AlGaN-based deep ultraviolet light-emitting diodes," *Micromachines*, vol. 14, no. 4, p. 844, 2023.